

NTUA 69/98
OUTP-98-10P
hep-lat/9802037

Dynamical Flavour Symmetry Breaking by a Magnetic Field in Lattice QED₃

K. Farakos and G. Koutsoumbas

National Technical University of Athens, Physics Department, Zografou Campus

GR-157 80, Athens, Greece,

and

N.E. Mavromatos*

University of Oxford, Department of (Theoretical) Physics, 1 Keble Road OX1 3NP,
Oxford, U.K.

Abstract

We perform a lattice study, in the quenched approximation, of dynamical mass generation in a system of relativistic (Dirac) fermions, coupled to an Abelian gauge field in (2+1)-dimensions, in the presence of an external (constant) magnetic field, perpendicular to the spatial planes. It is shown that a strong magnetic field catalyzes chiral symmetry breaking, in agreement with results in the continuum. The rôle of the higher-Landau poles in inducing a critical temperature above which the phenomenon disappears is pointed out. We also discuss the implications of this model on the opening of a gap in doped antiferromagnetic superconductors.

February 1998

(*) P.P.A.R.C. Advanced Fellow.

1 Introduction

In $(2+1)$ -dimensional gauge theories with relativistic fermions chiral symmetry can be defined only in the case of an *even* number of *massless* fermion species, $2N$, in the so-called 4×4 *reducible* Dirac formalism [1]. Fermion mass terms break the chiral symmetry $U(2N) \rightarrow U(N) \times U(N)$. To preserve parity one needs to have masses with opposite sign between the fermion species. This is the only type of mass terms that is allowed to be generated *dynamically* in *vector-like theories*, as a result of energetics arguments [2].

The problem of chiral symmetry breaking in $(2+1)$ -dimensional *continuum* QED_3 in the presence of *external magnetic fields* has been studied extensively in the recent literature [3, 4], following analyses in four dimensional gauge theories [5, 3, 6]. According to these findings, a strong enough magnetic field acts as a strong catalyst of chiral symmetry breaking, which occurs even in the limit of weak gauge couplings. We remind the reader that, in the absence of such strong fields, dynamical chiral symmetry breaking (i.e. fermion mass generation) occurs only in *supercritical theories* [1], i.e. for dimensionless gauge couplings that are stronger than some critical value g_c ¹. The effect of the strong magnetic field is, according to the analysis of [3, 6], to reduce g_c to zero. This phenomenon was termed in [3] *magnetic catalysis*.

This phenomenon may be important in the physics of high-temperature superconductivity, as pointed out in ref. [8]. Indeed, it is believed that high-temperature superconductors may have some strong connection with relativistic $(2+1)$ -dimensional gauge theories [9, 10, 11, 8]. This belief is enforced recently, as a result of experiments indicating that the high-temperature superconductivity is actually due to the opening of a *d*-wave gap in the hole (fermion) spectrum [12]. As is well known, *d*-wave superconductivity is characterized by lines of *nodes* of the gap. In the gauge theory approach to doped antiferromagnets, such hole (charged) excitations about such nodes are described by Dirac fermions [9, 11], coupled to gauge fields that describe the magnetic interactions among the charged degrees of freedom, in a spin-charge separating formalism [13].

The models of ref. [9, 8] describe the dynamical opening of a fermion gap at those nodes. Moreover, the theoretical analysis of [8] indicated that the dynamical fermion gap, due to the statistical gauge interactions, is enhanced in the presence of strong external magnetic fields, as expected from the general theory of [6, 3, 4]. The analysis of [8] also indicated the existence of a critical temperature above which chiral symmetry is restored in the model. This phase transition occurs well within the superconducting phase of the model and pertains only to the fermion gap at the nodes of the *d*-wave gap². For the

¹In $(2+1)$ -dimensions the effective dimensionless gauge coupling is actually the inverse of the fermion flavour number, $1/N$. Thus supercriticality in the coupling means actually the existence of a critical number of flavours N_c , below which dynamical chiral symmetry breaking is possible. Continuum Schwinger-Dyson analyses [1], in the large N approximation, have indicated that $N_c \simeq 32/\pi^2$. This result has also been argued to be correct on the basis of lattice analyses [7].

²We note that the problem of looking at charged fermions in the presence of an external field is compatible with the superconducting nature of the high-temperature superconductors. These materials are

model of [8], in the absence of external magnetic fields, the fermion gap at the nodes disappears at temperatures 0.1 K at most; in contrast, under the influence of a strong magnetic field $1 \text{ Tesla} < B < 20 \text{ Tesla}$, the fermion gap at the nodes remains up to temperatures of order 30 K.

It is worth pointing out that recent experiments have indicated the presence of such gaps at the nodes of a conventional d -wave gap [14]. Such experiments involved magnetic fields of the above order of magnitude, and they showed clearly the existence of a gap up to temperatures that are in close agreement with the above theoretical results. Although there may be alternative explanations for the phenomenon, the above qualitative agreement between theory and experiment prompts further studies of the magnetic catalysis phenomenon.

In addition to the above-mentioned motivation from Condensed Matter Physics, the study of the magnetic catalysis phenomenon in three-dimensional gauge theories is also useful from the point of view of high-temperature four-dimensional gauge theories in the Early Universe, or the physics of high-temperature quark-gluon plasma, in the presence of external fields, since both cases may be effectively described by three-dimensional gauge models.

Whatever the motivation might be, it becomes clear that the problem of the formation of a fermion condensate in the presence of strong external fields is quite relevant for physical applications. So far, as far as we are aware of, the analysis was restricted to the continuum formalism [3, 4]. It is the purpose of this work to present a first, preliminary, analysis of the phenomenon on the lattice, in the quenched approximation in the case of $(2+1)$ -dimensional *QED*.

We shall discuss here the formation of parity-invariant fermion condensates. In our analysis we shall trigger the phenomenon of chiral symmetry breaking by adding bare masses which preserve parity, and then extrapolate the results to the zero bare mass case. In this way we find only magnetically-induced condensates which preserve parity. Notice that in the presence of an external magnetic field, the theory ceases to be vector-like, and hence the theorem of [2] no longer applies, and one could in principle have parity-violating fermion condensates. This phenomenon was conjectured by Laughlin [15] as happening in the case of the high-temperature superconductors, offering a possible explanation of the results of the experiments of [14]. Our results in this work, though, indicate that parity-violating induced condensates might not be necessary for a possible explanation of the situation in the experiments of [14].

known to be strongly type II, which implies that the Meissner effect penetration depth in the superconducting phase is quite large, a few thousands of Angströms.

2 Results in the continuum from a novel perspective

In this section we describe briefly the theoretical formalism in the continuum [3, 4]. One follows essentially the method of Schwinger [16], by looking at the coincidence limit of the fermion propagator (in configuration space), $\text{Lim}_{x \rightarrow y} S(x, y)|_B$, in the presence of a constant external field, B . We start first from the free-fermion case, i.e. the case where the fermions interact only with the external constant field. The external gauge potential is then given by:

$$A_\mu = -Bx_2\delta_{\mu 1} \quad (1)$$

and the Lagrangian is:

$$L = \frac{1}{2}\bar{\Psi}(i\gamma^\mu(\partial_\mu - ieA_\mu^{ext}) - m)\Psi \quad (2)$$

where m is a *parity conserving* bare fermion mass, and the γ -matrices belong to the reducible 4×4 representation, appropriate for an even number of fermion species formalism [1, 9, 11].

The induced fermion condensate is given by the coincidence limit of the fermion propagator ³

$$\begin{aligned} <0|\bar{\Psi}\Psi|0>|_B &= +\text{Lim}_{x \rightarrow y} \text{tr}S(x, y)|_B \\ \text{where } S(x, y) &= <0|T\bar{\Psi}(x)\Psi(y)|0>|_B \end{aligned} \quad (3)$$

Following the proper time formalism of Schwinger [16], the propagator $S(x, y)|_B$ in the presence of a constant external magnetic field can be calculated exactly [3]:

$$\begin{aligned} S(x, y)|_B &= \exp\left(ie\int_x^y A_\mu^{ext} dz^\mu\right) \tilde{S}(x - y)|_B \\ \tilde{S}(x)|_B &= \int_0^\infty \frac{ds}{8(\pi s)^{3/2}} \exp\left[-i\left(\frac{\pi}{4} + sm^2\right)\right] \times \exp\left[-\frac{i}{4s}x_\nu C^{\nu\mu} x_\mu\right] \\ &\times \left[\left(m + \frac{1}{2s}\gamma^\mu C_{\mu\nu} x^\nu - \frac{e}{2}\gamma^\mu F_{\mu\nu}^{ext} x^\nu\right) \times \left(esB\cot(eBs) - \frac{es}{2}\gamma^\mu\gamma^\nu F_{\mu\nu}^{ext}\right)\right] \end{aligned} \quad (4)$$

where $F_{\mu\nu}^{ext}$ is the Maxwell tensor corresponding to the external background gauge potential (1), and $C_{\mu\nu} = \eta^{\mu\nu} + ([F^{ext}]^2)^{\mu\nu}[1 - eB\cot(eBs)]/B^2$, and the line integral is calculated along a straight line. A useful expression, to be used in the following, is the Fourier transform $\tilde{S}_E(k)|_B$ in Euclidean space of $\tilde{S}(x - y)|_B$ [3]:

$$\begin{aligned} \tilde{S}_E(k)|_B &= -i \int_0^\infty ds \exp\left[-s(m^2 + k_0^2 + k_\perp^2) \frac{\tanh(eBs)}{eBs}\right] \\ &\times \left\{[-k_\mu\gamma^\mu + m - i(k_2\gamma_1 - k_1\gamma_2)\tanh(eBs)] \times [1 - i\gamma_1\gamma_2\tanh(eBs)]\right\} \end{aligned} \quad (5)$$

We define

$$\Delta <\bar{\Psi}\Psi>|_B \equiv <0|\bar{\Psi}\Psi|0>|_B - <0|\bar{\Psi}\Psi|0>|_{B=0} \quad (6)$$

³We define for convenience the condensate with a plus sign, rather than the usual minus sign.

A straightforward calculation, then, yields in (2+1)-dimensional space-time the following result for $\Delta < \bar{\Psi} \Psi > |_B$ [3]:

$$\begin{aligned}
\Delta < \bar{\Psi} \Psi > |_B &= \frac{i}{(2\pi)^3} \int d^3 k t r [\tilde{S}_E(k)|_B - \tilde{S}_E(k)|_{B=0}] \\
&= \frac{4m}{(2\pi)^3} \int d^3 k \int_0^\infty ds [\exp\{-s(m^2 + k_0^2 + k_\perp^2 \frac{\tanh(eBs)}{eBs})\} - \exp\{-s(m^2 + k_0^2 + k_\perp^2)\}] \\
&= \frac{meB}{2\pi^{\frac{3}{2}}} \int_0^\infty ds \frac{e^{-sm^2}}{\sqrt{s}} [\coth(eBs) - \frac{1}{eBs}]
\end{aligned} \tag{7}$$

In the formulae above we have used the notations: $k_\perp^2 = k_1^2 + k_2^2$. The limit of the final expression as $m \rightarrow 0$ is easily found to be $\frac{eB}{2\pi}$. We note here that the infinities in $< \bar{\Psi} \Psi >$ are already present for zero magnetic field, so by performing the subtraction to form $\Delta < \bar{\Psi} \Psi > |_B$ we get an automatically finite result and there is no need to introduce explicit cut-offs in the integrals.

We show, in figure 1, the outcome of the numerical calculation of (7) for three different masses. The magnetic field in the following figures will be represented by the ratio $b \equiv \frac{eB}{\pi}$.

⁴ There is a striking result, depicted in this figure, namely that $\Delta < \bar{\Psi} \Psi > |_B$ increases for decreasing mass. This may be understood through the remark that the response of the system to an external field is bigger for small masses. An important point is that the value of this quantity has a finite limit as $m \rightarrow 0$, the value $\frac{eB}{2\pi}$, referred to above.

Further insight in the model, as well as the tools to investigate the finite temperature issue, is offered by the expansion of the propagators in terms of the Landau level contributions. The relevant expansion reads:

$$\tilde{S}_E(k)|_B = -ie^{\frac{-k^2}{eB}} \sum_{n=0}^{\infty} (-1)^n \frac{D_n(m, B, k)}{k_0^2 + M_n^2(B)}, \tag{8}$$

with $M_n^2(B) \equiv m^2 + 2eBn$ and $Tr D_n(m, B, k) = 4m[L_n(\frac{2k_\perp^2}{eB}) - L_{n-1}(\frac{2k_\perp^2}{eB})]$.

We need the integrals over the momenta k_1, k_2 , which are calculated using the formula:

$$\int dk_1 dk_2 e^{-\frac{k^2}{eB}} [L_n(\frac{2k_\perp^2}{eB}) - L_{n-1}(\frac{2k_\perp^2}{eB})] = (-1)^n 2\pi eB. \tag{9}$$

What is left is the sum over the k_0 momentum. We consider the case of zero temperature (the case we have just treated), which means one should perform the integral over k_0 . The result reads:

$$< \bar{\Psi} \Psi > |_B = \frac{eB}{2\pi} + \frac{emB}{\pi} \sum_{n=1}^{\infty} \frac{1}{M_n(B)} = \frac{eB}{2\pi} - \frac{m\sqrt{2eB}}{2\pi} \zeta(\frac{1}{2}, \frac{m^2}{2eB}) \tag{10}$$

⁴The denominator π has been included here to facilitate the comparison with the lattice results: there the quantity b is defined as the ratio $\frac{eB}{eB|_{max}}$, where $eB|_{max}$ is the maximum magnetic field (in lattice units) that can be achieved on the lattice; this maximal value is π .

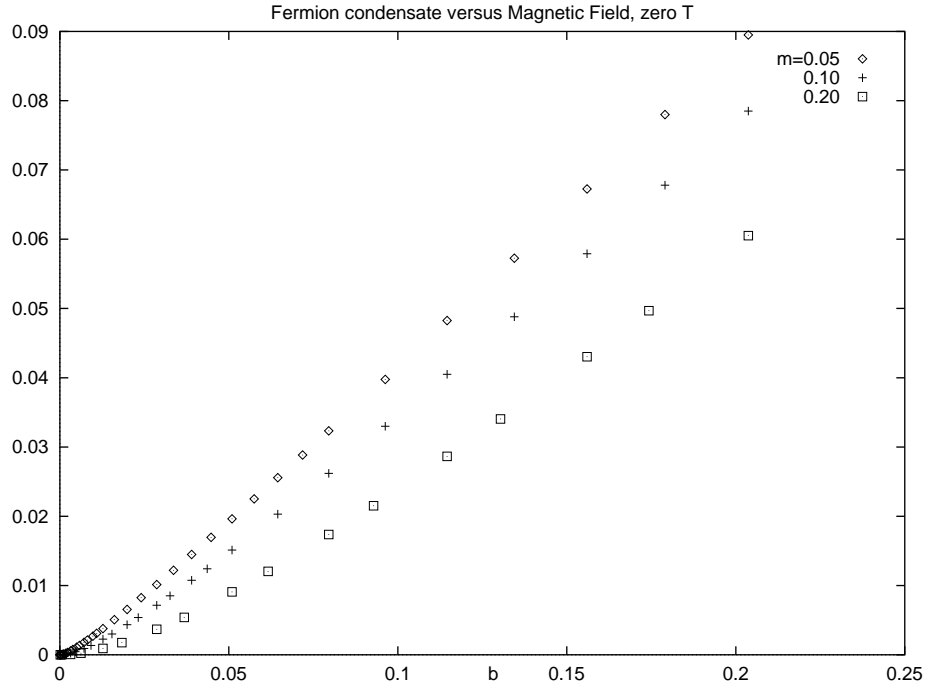


Figure 1: $\langle \bar{\Psi} \Psi \rangle$ versus $\frac{eB}{\pi}$ at zero temperature

where $\zeta(z, q)$ is one of the Riemann ζ functions, which is understood to be defined through appropriate analytic continuation [17]. The first term in the middle part of the equality (10) is mass independent and coincides with the previous result in the massless limit, while the remaining part of the expression vanishes in this limit. Thus, for the zero-temperature case, we find that in three dimensional gauge theories a strong magnetic field (such that $|eB|$ is much larger than any other mass scale in the problem), may induce a fermion gap⁵.

It is worthy of examining some physically interesting limiting cases of (10), keeping however eB finite. First, consider the case of weak magnetic fields (compared to the (bare) fermion mass m): $eB \ll m^2$. In that case one may expand $M_n^{-1} \simeq m^{-1} \left(1 - \frac{eB}{m^2} n + \dots \right)$. The resulting sums can be regularized by means of the Riemann's second ζ function, $\zeta(z) = \sum_{n=1}^{\infty} n^{-z}$, using [17]: $\zeta(0) = -\frac{1}{2}$, $\zeta(-1) = -1/12$ (both being understood by

⁵Notice an important difference from the corresponding four-dimensional problem, where the corresponding fermion condensate reads:

$$\langle \bar{\Psi} \Psi \rangle \sim -|eB| \frac{m}{4\pi^2} \left(\ln \frac{\Lambda^2}{m^2} + \mathcal{O}(m^0) \right) \rightarrow 0 \quad ; \quad m \rightarrow 0 \quad (11)$$

and tends to zero as the bare mass $m \rightarrow 0$, for a fixed (ultraviolet) scale Λ . However, the quantum dynamics of the electromagnetic field may drastically change the situation if treated non-perturbatively [3, 6].

means of appropriate analytic continuation). The result is:

$$\Delta \langle \bar{\Psi} \Psi \rangle |_{eB \ll m^2} \simeq \frac{(eB)^2}{12m^2\pi} + \dots \quad (12)$$

with the \dots indicating subleading terms of higher order in eB/m^2 . Thus, for weak magnetic fields the induced gap scales quadratically with the external field intensity, for massive fermions.

In a similar manner, for strong magnetic fields $eB \gg m^2$, one finds

$$\Delta \langle \bar{\Psi} \Psi \rangle |_{eB \gg m^2} \simeq \frac{(eB)}{2\pi} \left(1 + \zeta\left(\frac{1}{2}\right) \frac{\sqrt{2}m}{\sqrt{eB}} - \frac{\sqrt{2}m^3}{[eB]^{3/2}} \zeta\left(\frac{3}{2}\right) + \dots \right) \quad (13)$$

where $\zeta\left(\frac{1}{2}\right) \simeq -1.46$, $\zeta\left(\frac{3}{2}\right) \simeq +2.61$. Notice that despite the fact that the various terms in (13) come with alternating signs, however *there is no critical value* of the field, consistent with the approximation $m/\sqrt{eB} \ll 1$, at which the condensate in (13) *changes sign*.

We now come to the model at finite temperature. The integral over k_0 should be replaced by a sum over $k_0 = 2\pi(n + \frac{1}{2})T$. The $T = 0$ result is modified to:

$$\langle \bar{\Psi} \Psi \rangle |_T = \frac{eB}{2\pi} \tanh\left(\frac{m}{2T}\right) + \frac{emB}{\pi} \sum_{n=1}^{\infty} \frac{1}{M_n(B)} \tanh\left(\frac{M_n(B)}{2T}\right), \quad (14)$$

thereby implying the *absence* of the condensate for *any finite temperature* if the bare infrared cut-off mass m , for finite constant B .

In a similar fashion, as for the zero-temperature case, one may perform the summation over the Landau poles for certain limiting cases. The physically interesting case is the one for which one assumes a strong field $eB \gg m^2$ and a temperature regime $T \gg m$, but such that $eB \gg T^2$. In such a case $\tanh(M_n(B)/2T) \simeq 1$ for all n , whilst $M_n(B) \simeq \sqrt{2eBn}$, to leading order. Hence,

$$\Delta \langle \bar{\Psi} \Psi \rangle |_T \simeq \frac{eB}{4\pi} \frac{m}{T} - \frac{1.46m\sqrt{eB}}{\sqrt{2}\pi} \quad (15)$$

using $\zeta(1/2) = -1.46$. Notice the existence of a *critical temperature*, for non-zero m ,

$$T_c \simeq \frac{1}{4} \sqrt{eB} \quad (16)$$

above which the condensate vanishes⁶. The order of magnitude of the temperature is consistent with the approximations made in the derivation of (16), which suggests an

⁶To be precise, at $T = T_c$ the condensate changes sign. However, given that in three-dimensional gauge theories $\langle \bar{\Psi} \Psi \rangle \propto E^2$, with E the (magnetically-enhanced) fermion energy gap, such a change in sign is interpreted as implying that above T_c thermal fluctuations dominate, and, hence, prevent chiral symmetry breaking. It is in this sense that we used above the terminology ‘critical temperature’.

important rôle for the higher Landau levels at finite temperatures,⁷ namely that they prevent dynamical mass generation above a certain temperature. This is consistent with the fact that for $B \rightarrow \infty$, where only the lowest Landau poles are retained, there is dynamical mass generation for all $T < \infty$. In the context of a possible application of this phenomenon to high-temperature superconductors [8], we note that \sqrt{eB} scaling of a critical temperature with the external field intensity are reported in the experiments of [14]. Notice however, that the existence of extra interactions, that may lead to dynamical mass generation for fermions, as in the $SU(2) \times U_S(1)$ model of [11], the scaling of the critical temperature with B may be different [8].

We now proceed with a different regularization, based on the remark that all infinities in the model lie in the $T = 0$ sector, so that the difference

$$\langle \bar{\Psi} \Psi \rangle |_T - (\langle \bar{\Psi} \Psi \rangle |_{T=0}) = \frac{eB}{\pi} \frac{1}{1 + e^{\frac{m}{T}}} - \frac{2emB}{\pi} \sum_{n=1}^{\infty} \frac{1}{M_n(B)} \frac{1}{1 + e^{\frac{M_n(B)}{T}}}, \quad (17)$$

of the condensate at finite temperature, as given by (14), and its zero temperature limit should be finite. On the other hand, the zero temperature part has already been regularized above by the subtraction of the $B = 0$ part and the finite result is given in equation (7). Thus, we may calculate $\Delta \langle \bar{\Psi} \Psi \rangle |_T$ substituting for $\Delta \langle \bar{\Psi} \Psi \rangle |_{T=0}$ the regularized expression of (7) and for the finite difference the series of (17). The result of these calculations is depicted in figure 2.

We have used two masses, $m = 0.20$ and $m = 0.05$. We remark that the regularization scheme we have adopted seems to work quite well. We observe that (say for the larger mass, where the effects are more transparent) one may distinguish three temperature regimes, delimited by $\tau_1 \equiv Ta \simeq 0.04$ and $\tau_2 \equiv Ta \simeq 0.17$. Below τ_1 the condensate is the same as for zero temperature, thus if one uses lattices of time extent equal roughly to $\frac{1}{\tau_1}$, which equals about 25 in the $m = 0.20$ case, one should get zero temperature results. After that the condensate starts decreasing and vanishes at τ_2 . Thus, for lattices with temporal extent of about $\frac{1}{\tau_2}$ (about 6 in the $m = 0.20$ case) one should expect the vanishing of the condensate. For the smaller value of the mass, 0.05, the zero temperature value is larger, in agreement with the results in figure 1, but it decreases more steeply. The corresponding values for τ_1 and τ_2 are 0.01 and 0.145 respectively, yielding the corresponding temporal extents 100 and 7. Comparing the results for the two masses we observe that for small temperatures (corresponding to large enough lattices) the condensate for the smallest masses are the largest, as explained in figure 1; however, if the lattice is relatively small, corresponding to a high temperature, it is expected that the condensates for the “big” masses will take over. This could be used as a check that the lattice size used is large enough.

⁷Especially as far as the superconductivity phenomenon is concerned, there is a natural upper bound for the magnetic field, B_c , above which superconductivity is destroyed. For realistic cases, the critical field in the high-temperature superconducting oxides is of order of 20 Tesla. For such fields the inclusion of the higher Landau poles seems necessary.

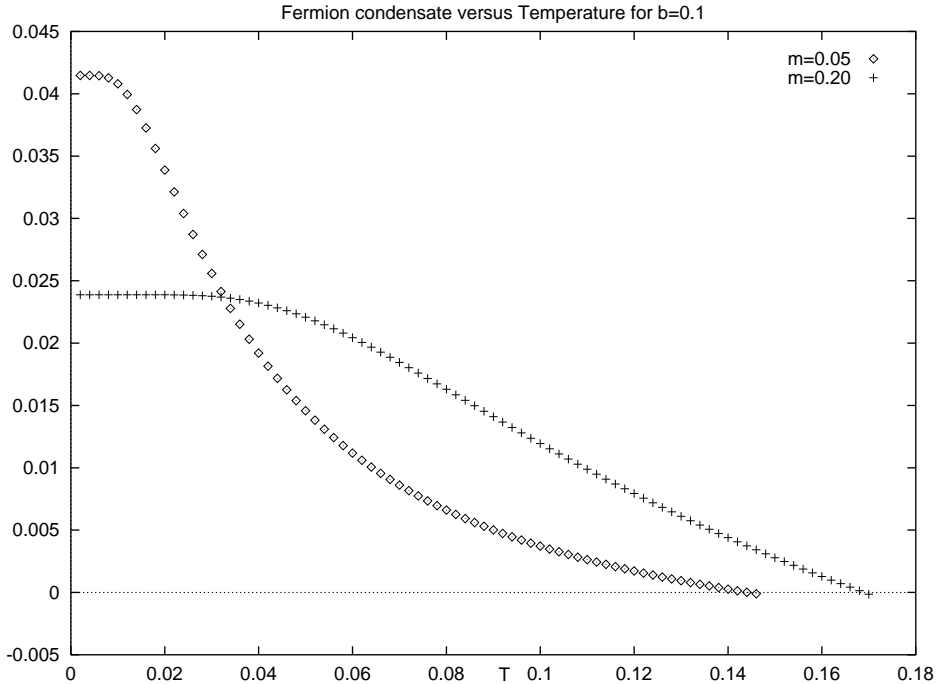


Figure 2: $\langle \bar{\Psi} \Psi \rangle$ versus temperature at fixed magnetic field

We have plotted the value of the critical temperature T_c (denoted by τ_2 above) versus the magnetic field in figure 3.

We have used data for two masses and performed a square root fit: $T_c = \kappa(m)\sqrt{b} = \frac{\kappa(m)}{\sqrt{\pi}}\sqrt{(eB)}$. It turns out that $\kappa(0.05) = 0.46$ and $\kappa(0.20) = 0.52$, so that $\frac{\kappa(0.05)}{\sqrt{\pi}} \simeq 0.26$, $\frac{\kappa(0.20)}{\sqrt{\pi}} \simeq 0.29$. We observe that the fit is better for the small mass, which is quite reasonable, since the square root behaviour has been found in the limit of big magnetic field as compared to the mass squared. The big values of the magnetic field have been fitted, so the discrepancies occurring in for the bigger mass take place at small magnetic fields. The proportionality constants 0.26 and 0.29 given by this approach is equal to a very good approximation with the value $\frac{1}{4}$ yielded by the ζ function regularization (16), applicable when the magnetic field is strong. We note that strong field means value of the ratio $\frac{eB}{m^2}$ much greater than 1. In the case we are considering, the value $b = 0.1$ corresponds to $\frac{eB}{m^2} \simeq 8$, for $m=0.20$ and to $\frac{eB}{m^2} \simeq 128$, for $m=0.05$. Thus the two different approaches agree quite well and reproduce the magnetic field dependence found experimentally.

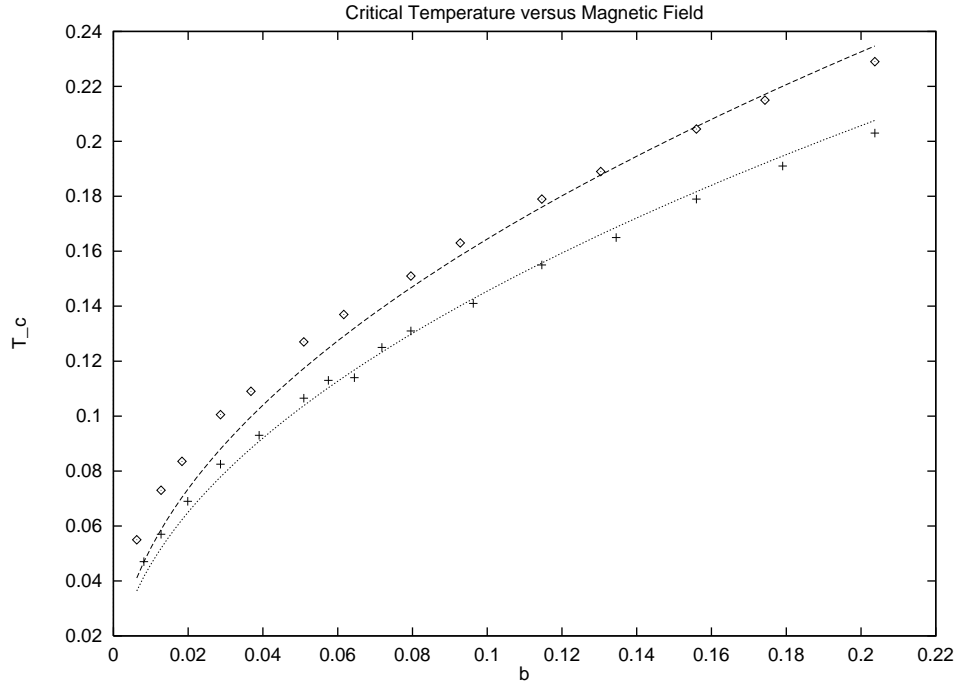


Figure 3: Critical temperature versus magnetic field for two masses: the upper data and fit correspond to $m = 0.20$, the lower data and fit to $m = 0.05$.

3 The Lattice Model

We now describe briefly the field-theoretical model associated to the problem of superconductivity as formulated above. The relevant three-dimensional Lagrangian is:

$$L = -\frac{1}{4}(f_{\mu\nu}^S)^2 + \bar{\Psi}D_\mu\gamma_\mu\Psi - m\bar{\Psi}\Psi, \quad (18)$$

with D_μ the covariant derivative. The field strength corresponds to the “statistical” gauge field α_μ^S . The mass term has been introduced by hand to facilitate the lattice treatment and the limit $m \rightarrow 0$ will be considered in the end. It has already been explained that the Clifford algebra is reducible in three dimensions and the model may also be represented by 2×2 matrices acting on two species of fermions with opposite mass parameters. The generators $\mathbf{1}$, γ_3 , γ_5 and $\Delta \equiv i\gamma_3\gamma_5$ generate a global $SU(2) \times U(1)$ symmetry of the Lagrangian (if m is set to zero). We observe that one may write down two kinds of mass term: the parity conserving mass term $m_C\bar{\Psi}\Psi$ and the parity violating one: $m_V\bar{\Psi}\Delta\Psi$. It is easy to see that the parity conserving mass term breaks the global $SU(2)$ symmetry, while the parity violating mass is an $SU(2)$ singlet. The $U(1)$ field acting on the fermions may consist of two parts, the electromagnetic $U_E(1)$, generated by an external electromagnetic potential A_μ , and the aforementioned statistical $U_S(1)$, associated with α_μ^S , responsible for the fractional statistics of the holon excitations of the doped antiferromagnet.

The model with an external homogeneous magnetic field has been examined in [3] in the two-component formalism for the fermions; it was found that the (parity violating) magnetic field gives rise to parity violating mass terms with opposite signs for the two fermion species. Thus, in the four-component formalism, the dynamically generated parity violating mass terms are expected to sum up to zero. On the other hand, the effect of mass generation will manifest itself in an enhancement of the parity conserving mass, as compared to the free fermion field case.

We would like to study the above effects by lattice methods; this will free us from the need of the approximations used in [3] and will permit us to include the statistical gauge field, on top of the external electromagnetic field. The lattice action, corresponding to the continuum Lagrangian, may be written as:

$$S = \beta_G \sum_P (1 - \text{Tr} U_P) + \sum_{n,n'} \overline{\Psi}_n Q_{n,n'} \Psi_{n'} \\ Q_{n,n'} = \delta_{n,n'} - K \sum_{\hat{\mu}} [\delta_{n',n+\hat{\mu}}(r + \gamma_{\hat{\mu}}) U_{n\hat{\mu}} V_{n\hat{\mu}} + \delta_{n',n-\hat{\mu}}(r - \gamma_{\hat{\mu}}) U_{n-\hat{\mu}}^\dagger V_{n-\hat{\mu}}^\dagger]. \quad (19)$$

The indices n, n' are triples of integers, such as (n_1, n_2, n_3) , labeling the lattice sites, while μ denotes directions. r is the Wilson parameter, K the hopping parameter, $U_{n\hat{\mu}} \equiv e^{iga\alpha_{n\hat{\mu}}^S}$, $V_{n\hat{\mu}} \equiv e^{ieaA_{n\hat{\mu}}}$, with $\alpha_{n\hat{\mu}}^S$ the statistical gauge potential and $A_{n\hat{\mu}}$ the external electromagnetic potential. U_P is the product of the links surrounding a plaquette, as usual, and β_G is related to the three dimensional $U_S(1)$ coupling constant by $\beta_G = \frac{1}{g^2 a}$, while we denoted by e the four dimensional (dimensionless) electromagnetic coupling of $U_E(1)$. In our treatment we will use naive Wilson fermions, so we set $r = 0$.

On the other hand, we would like to impose an external homogeneous magnetic field in the (missing) x_3 direction, thus we choose the external gauge potential in such a way that the plaquettes in the $x_1 x_2$ plane equal B , while all other plaquettes equal zero. This may be achieved in several ways, related with each other by gauge transformations. The value of B is restricted, due to the fact that the flux through the entire $x_1 x_2$ section of the lattice should equal an integer multiple of 2π , so for the $x_1 x_2$ plane with area N^2 we have: $B = \frac{2\pi}{N^2} l$, with l some integer between 0 and $\frac{N^2}{2}$. (The model with integers l between $\frac{N^2}{2}$ and N^2 is equivalent to the model with integers $N^2 - l$ which fall into the previous category.) We remark here that the maximum value the magnetic field B can take is π . The physical magnetic field B_{phys} is related to B through $B = e\alpha^2 B_{\text{phys}}$, and the physical field may go to infinity, as it should, if the lattice spacing α goes to zero, while B is kept constant.

However, the above considerations are complicated by the fact that the lattice is a torus, that is a closed surface, and the Maxwell equation $\text{div} \mathbf{B} = 0$ implies that the magnetic flux through the lattice should vanish. This means that, if periodic boundary conditions are used for the gauge field,⁸ the gauge field configuration will have zero total

⁸An alternative way out might be, of course, the use of twisted boundary conditions.

flux, so the (positive, say) flux B , penetrating the majority of the plaquettes, will be accompanied by a compensating negative flux in a small number of plaquettes. This point will become clear in a while.

To begin with, we consider a configuration giving flux B in each plaquette. In analogy with the continuum, one would consider something like: $aeA_1 = -Bn_2$, $A_2 = 0$, $A_3 = 0$, with $B = \frac{2\pi}{N^2}l$. However, due to the periodic boundary conditions, the plaquettes in the x_1x_2 plane starting at the point (n_1, n_2) with $n_2 = N$, will not have flux equal to B . To cure this, one modifies a little bit the configuration by demanding $aeA_2 = B(Nn_1 - \frac{N}{2} - \frac{N^2}{2})$, whenever $n_2 = N$. Thus, all the plaquettes have now flux equal to B , with the exception of the one starting at $(n_1 = N, n_2 = N)$. This plaquette is characterized by flux equal to $-B(N^2 - 1)$, which is exactly what is needed to cancel the contribution of all other plaquettes. We remind the reader that the value of these plaquettes does not depend on x_3 , so, considering the three-dimensional configuration, we have a constant flux through the $N^2 - 1$ plaquettes and a “Dirac string” of flux of opposite sign through the (N, N) plaquette for every x_3 .

What we would like to study is the $\langle \bar{\Psi}\Psi \rangle$ condensate, which will depend on the lattice point in which it will be calculated. The dependence will be very small if one uses sites deep inside the region where the magnetic field is homogeneous. One should expect a strong dependence on the site near the location of the string of the large negative flux. We have measured the condensate in the middle of the lattice. Another concern is the kind of boundary conditions one will use for the fermions. In the time direction we used antiperiodic boundary conditions, conforming to common practice. For the spatial directions one may use periodic or fixed boundary conditions (the latter meaning that the fermion fields vanish on the boundaries). We have used both and found out that the results agree for large enough lattices. Finally we chose to work with the fixed boundary conditions, so that the fermion matrix feels the least influence from the big negative flux, which is located exactly on the boundary.

4 Lattice Results

We start with the treatment of the model in the limit $\beta_G \rightarrow \infty$, that is we consider the case where the statistical gauge potential is frozen to zero. In this case, the action simplifies to:

$$S = \sum_{n,n'} \bar{\Psi}_n Q_{n,n'} \Psi_{n'} \\ Q_{n,n'} = \delta_{n,n'} - K \sum_{\mu} [\delta_{n',n+\hat{\mu}} \gamma_{\mu} e^{igaA_{n\mu}} - \delta_{n',n-\hat{\mu}} \gamma_{\mu} e^{-igaA_{n-\hat{\mu},\mu}}], \quad (20)$$

where

$$aeA_1 = -Bn_2, \quad aeA_2 = \delta_{n_2 N} B(Nn_1 - \frac{N}{2} - \frac{N^2}{2}), \quad A_3 = 0,$$

as explained above. We now explain some analytical aspects which may give further insight into the model and help us to have an independent check of our results in this case. We note that for large enough lattices one may disregard the boundary effects, if the condensate is measured away from the regions of inhomogeneity, as explained above. Then the gauge field configuration is simplified to:

$$aeA_1 = -Bn_2, \quad A_2 = 0, \quad A_3 = 0,$$

and the action is further reduced to the form:

$$\begin{aligned} S = \sum_{n,n'} \bar{\Psi}_n Q_{nn'} \Psi_{n'} \\ Q_{nn'} = \delta_{nn'} - K\gamma_1(\delta_{n',n+1} e^{-iBn_2} - \delta_{n',n-1} e^{iBn_2}) - \\ K\gamma_2(\delta_{n',n+2} - \delta_{n',n-2}) - K\gamma_3(\delta_{n',n+3} - \delta_{n',n-3}) \end{aligned} \quad (21)$$

We observe from (21) that in order to take the continuum limit of the lattice action, one should consider B on the lattice, such that the maximum BN of Bn_2 should satisfy $\sin BN \simeq BN$, which implies that ⁹ the magnetic field B should be small enough. If we would like a somewhat more quantitative estimate of the maximum allowed magnetic field, a trivial calculation of the cyclotron radius can indicate that for $B \simeq \frac{\pi}{8}$ this radius equals two lattice spacings and it decreases for increasing B . Thus the wave functions are expected to have structure at distances smaller than one lattice spacing and the discretization becomes important. Thus it seems reasonable to stop at this value of B .

A semi-analytical evaluation of the fermion condensate $\langle \bar{\Psi}_{(0n_20)} \Psi_{(0n_20)} \rangle$ is achieved by first taking the Fourier transform of $Q_{n_2 n'_2}$ for the directions 1 and 3, and then inverting $Q_{n_2 n'_2}$:

$$\langle \bar{\Psi}_{(0n_20)} \Psi_{(0n_20)} \rangle = \frac{1}{NN_\tau} \sum_{p_1, p_3} \left(\frac{1}{Q} \right)_{n_2 n_2} \quad (22)$$

$$Q_{n_2 n'_2} = \delta_{n_2 n'_2} - 2iK\gamma_1 \sin(p_1 + Bn_2) \delta_{n_2 n'_2} - 2iK\gamma_3 \sin(p_3) \delta_{n_2 n'_2} - K\gamma_2(\delta_{n'_2, n_2+1} - \delta_{n'_2, n_2-1}). \quad (23)$$

The quantities p_1 and p_3 in the sum take the values $\frac{2\pi}{N}n_1$ and $\frac{2\pi}{N_\tau}(n_3 + \frac{1}{2})$ respectively. We remark here that this approach parallels the one of Landau when he first derived the Landau levels for the motion of a particle in a homogeneous external magnetic field. We have checked that the results from the full lattice calculation and the ones from the procedure outlined in (23) agree perfectly.

In figures 4 and 5 we plot $\Delta \langle \bar{\Psi} \Psi \rangle \equiv \langle \bar{\Psi} \Psi \rangle|_B - \langle \bar{\Psi} \Psi \rangle|_{B=0}$ versus the magnetic field B . In this and the following figures we use the ratio b , defined by $b \equiv \frac{eB}{eB|_{max}}$. Note that $eB|_{max} = \pi$ (recall the discussion after equation (19)).

Figure 4 shows the behaviour of $\Delta \langle \bar{\Psi} \Psi \rangle$, when the mass parameter m is 0.05 for various lattice volumes. We see clearly very strong volume effects, as expected for this

⁹We thank G. Tiktopoulos for a useful discussion on this point.

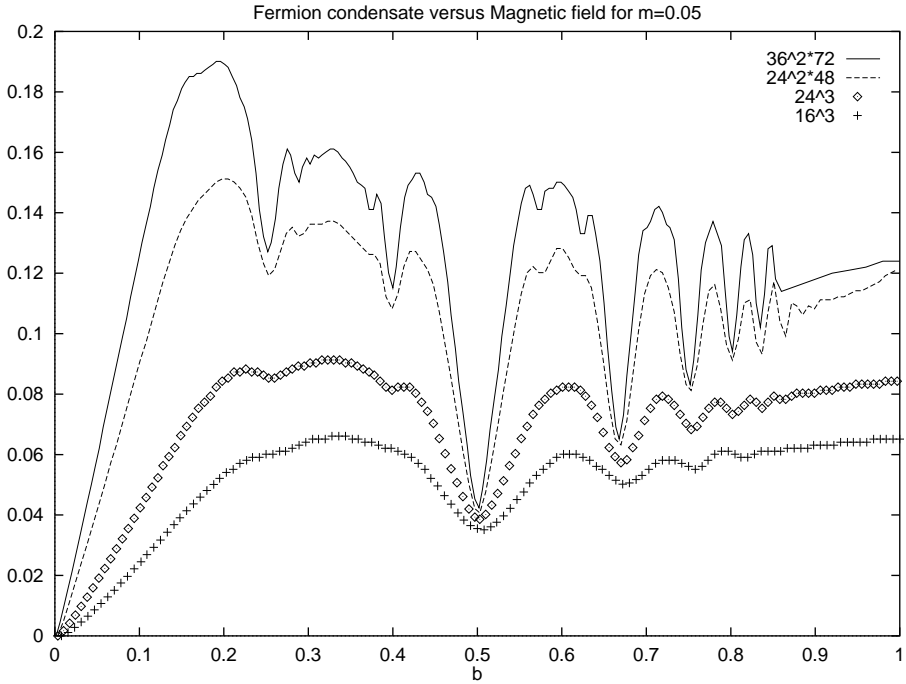


Figure 4: $\Delta \langle \bar{\Psi} \Psi \rangle$ versus the magnetic field for $m = 0.05$ and various volumes.

small mass value. As explained in figure 2, the lattice size should be around 100, if one is to get strictly zero temperature results. We see that the condensate keeps increasing with the volume. The finite temperature effects are stressed emphatically through the comparison of the results for the 24^3 and $24^2 \times 48$ lattices. We should note that we expect a non-trivial wave function renormalization of the composite operator $\langle \bar{\Psi} \Psi \rangle$, which can probably account for the difference in the values of the condensate as shown in figures 1 and 2 on one side and figure 4 on the other. The small B region has qualitatively the same behaviour as the corresponding result in figure 1. One may also observe the complicated behaviour for large magnetic fields, which is clearly a lattice artifact, as explained previously.

Figure 5 depicts the mass dependence of $\Delta \langle \bar{\Psi} \Psi \rangle$: Two masses ($m = 0.20, 0.10$) have been used. For $m = 0.20$ two different volumes have been used ($24^2 \times 48$ and $36^2 \times 72$). We recall from the discussion in figure 2 that for lattices of linear extent 25 or higher we should get zero temperature results. This is really what is clearly seen in figure 5: the two lattices, assumed large enough for this mass, give identical results. We have also plotted the results for $m = 0.10$ on the same figure. Two facts have to be pointed out: a) In the small B region we see that the condensates for $m = 0.10$ are bigger than the ones for $m = 0.20$, as anticipated in figure 1. b) The condensates go to zero with the mass for fixed volume. This just means that to get meaningful results one should first take the thermodynamic limit and after that the massless limit.

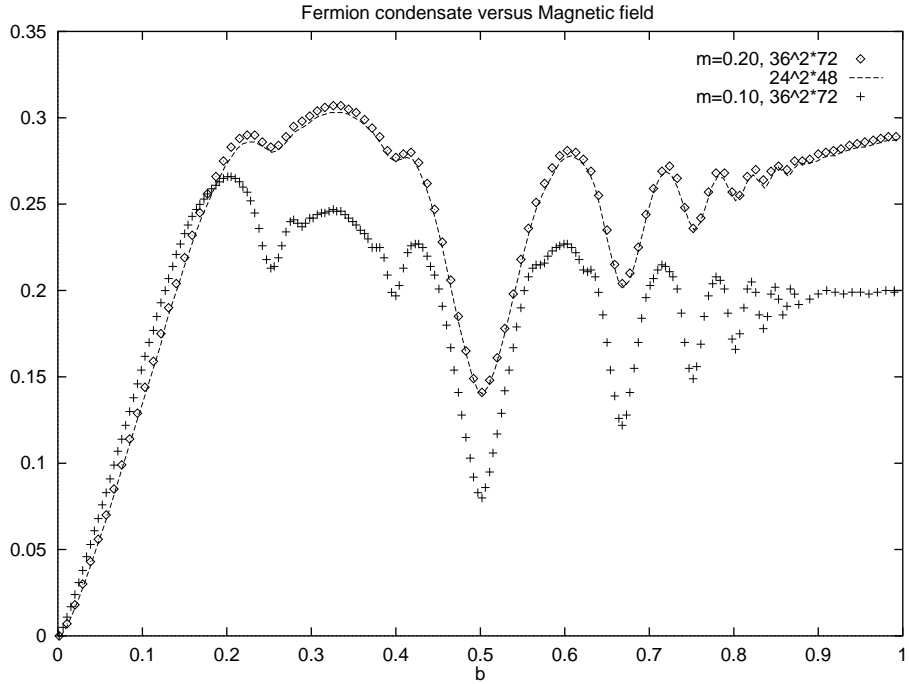


Figure 5: $\Delta <\bar{\Psi}\Psi>$ versus the magnetic field for $m = 0.10$ and $m = 0.20$.

Another issue that has to be settled is gauge invariance, in the sense that the various gauge potentials that may be used to generate a homogeneous magnetic field are equivalent. In figure 6 we show the result for the condensate for two gauge choices: $A_1 = -Bn_2$, $A_2 = 0$, $A_3 = 0$, and $A_1 = -\frac{Bn_2}{2}$, $A_2 = \frac{Bn_1}{2}$, $A_3 = 0$. Lattice volumes 6^3 and 16^3 have been used. We observe an approximate gauge invariance for the small volume and exact gauge invariance for the large volume. The discrepancy in the small volume has to do with the fact that only approximate gauge invariance can be achieved on small lattices, which are most sensitive to the boundary conditions.

After the discussion on the free fermion case, we next proceed to incorporate quantum fluctuations of the gauge field in the analysis.

As a first step, we show in figure 7 the condensate for zero magnetic field versus the mass m for a 16^3 lattice and three values of the gauge coupling β_G : 1, 3 and infinite (the latter corresponds to the free field). The value 1 is in the strong coupling regime, where a condensate will be formed dynamically, while the value 3 is in the weak coupling region, where the condensate is small (could be zero if we had dynamical flavors with more than four flavours). We observe that the values for $\beta_G = 3$ are very close to the ones for the free field theory; the extrapolation to zero mass for $\beta_G = 3$ will yield a very small value. On the other hand, the condensate for $\beta_G = 1$ are impressively big, signalling the breakdown of the global $SU(2)$ symmetry; the extrapolation to the massless limit certainly points to a non-zero value. We should point out here that we should subtract the perturbative

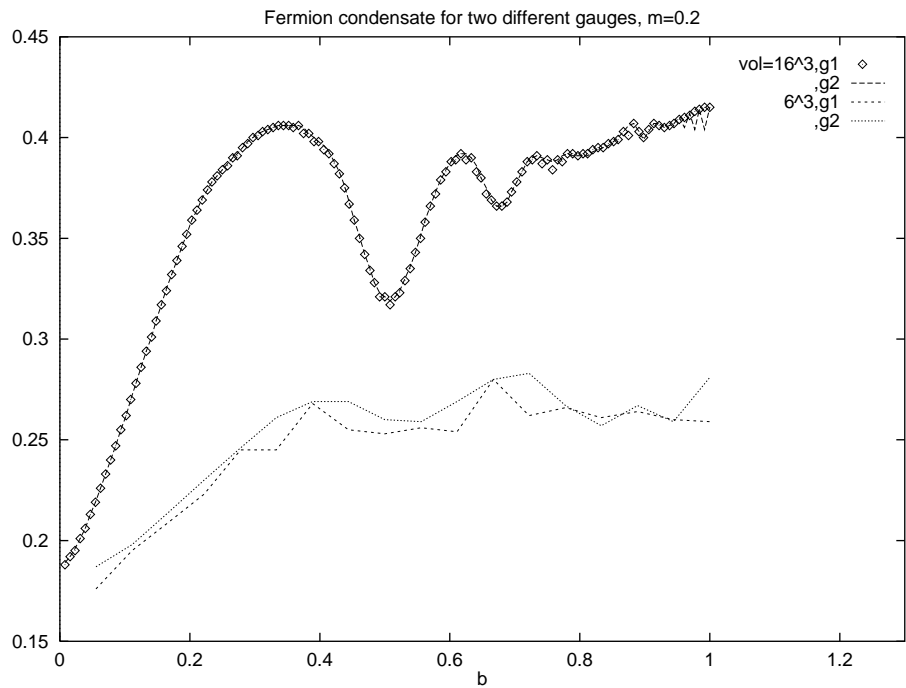


Figure 6: $\langle \bar{\Psi} \Psi \rangle$ versus the magnetic field for two gauge choices and two lattice volumes.

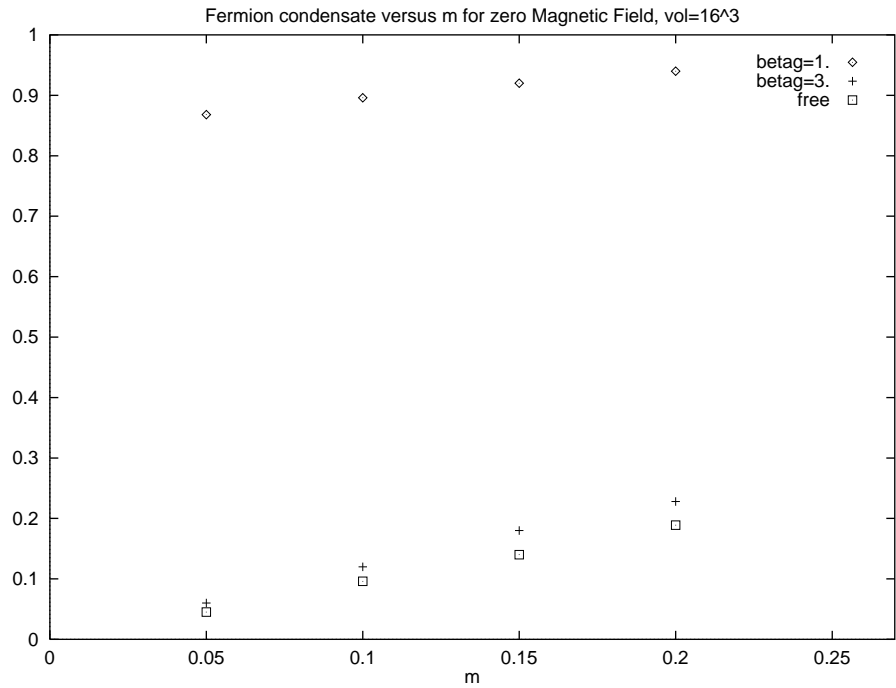


Figure 7: $\langle \bar{\Psi} \Psi \rangle$ versus m for zero magnetic field and three values of the gauge coupling.

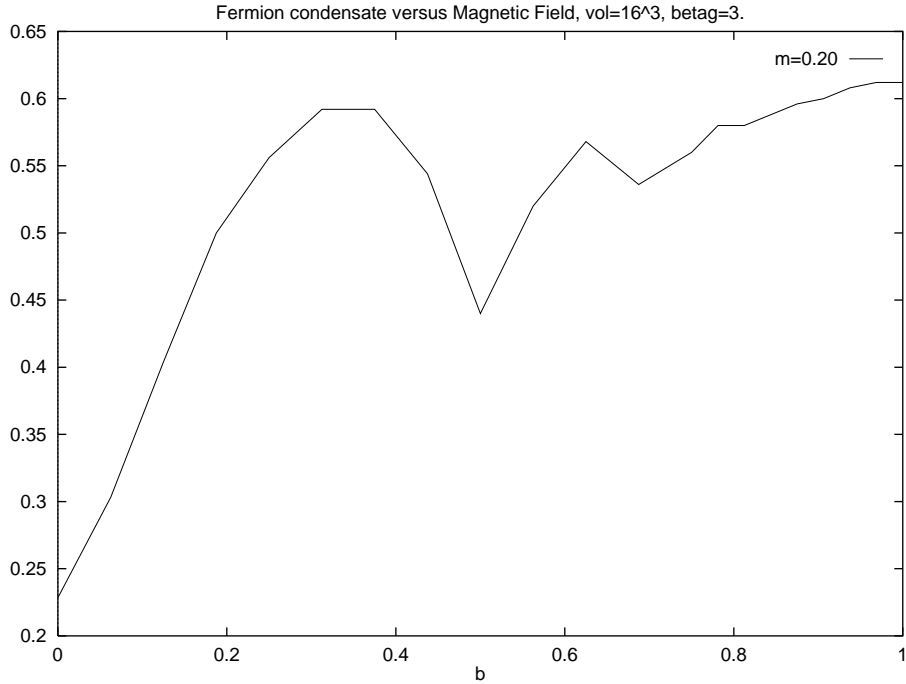


Figure 8: $\langle \bar{\Psi} \Psi \rangle$ versus the magnetic field for $m = 0.20$ and $\beta_G = 3$, for a 16^3 lattice.

contribution from our lattice result. In that sense our result is preliminary, since it lacks the perturbative calculation. We plan to include this in a future publication.

In the last two figures we depict the results for the full model versus the magnetic field. In figure 8 one may see the 16^3 result for $\beta_G = 3$, $m = 0.20$. These results should be compared against the ones in figure 6 for $V = 16^3$, $\beta_G = 3$, $m = 0.20$. They are obviously very similar, as expected.

In figure 9 we show the results for 16^3 lattice, $\beta_G = 1$ and $m = 0.20, 0.10, 0.05$. We observe the same qualitative behaviour with the free case in the small B region. However there is a crucial difference: a non-zero condensate is formed, *however small the bare mass may be*, because of the gauge interaction. On the other hand, we find an impressive smoothening out of the graph in the large B region; moreover, the difference between the results for the various masses decrease with increasing B , so, taken at face value, these results imply mass independence of the results in the large B region, as expected on the basis of the continuum results. However, in this region we expect many lattice artifacts, as explained before, so one should be careful with the interpretation of the subtle continuum limit.

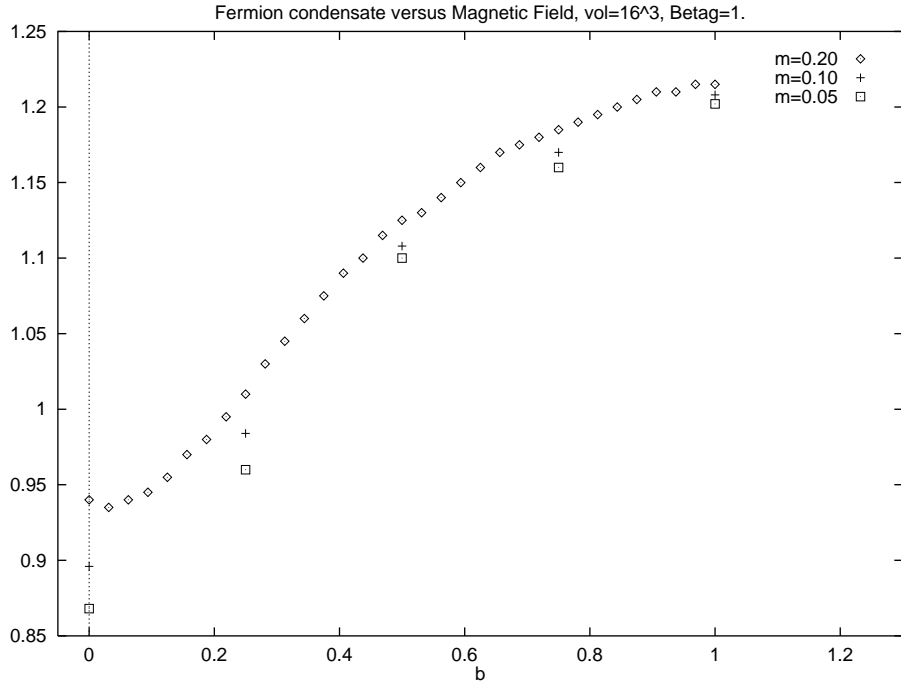


Figure 9: $\langle \bar{\Psi} \Psi \rangle$ versus m for zero magnetic field for $m = 0.20$, $m = 0.10$, $m = 0.05$ and $\beta_G = 1$, for a 16^3 lattice.

Acknowledgements

The authors wish to thank G. Tiktopoulos for valuable discussions. G.K. wishes to acknowledge partial financial support from PENED 95 Program No. 1170 of the Greek General Secretariat of Research and Technology. K.F. wishes to thank the TMR project number FMRX-CT97-0122 for partial financial support.

References

- [1] R. D. Pisarski, *Phys. Rev.* **D29** (1984), 2423;
 T. W. Appelquist, M. Bowick, D. Karabali and L. C. R. Wijewardhana, *Phys. Rev.* **D33** (1986), 3704.
 T. W. Appelquist, D. Nash and L. C. R. Wijewardhana, *Phys. Rev. Lett.* **60** (1988), 2575.
- [2] C. Vafa and E. Witten, *Comm. Math. Phys.* **95** (1984), 257.
- [3] V.P. Gusynin, V.A. Miransky and I.A. Shovkovy, *Phys. Rev. Lett.* **73** (1994), 3499;
Phys. Rev. **D52** (1995), 4718; *Nucl. Phys.* **B462** (1996), 249.

- [4] A.V. Shpagin, preprint hep-ph/9611412.
- [5] A.Chodos, K.Everding and D.A.Owen, *Phys. Rev.* **D42** (1990), 2881.
- [6] D.K. Hong, Y. Kim and S.J. Sin, *Phys. Rev.* **D 54** (1996) 7879;
 C.N. Leung, Y.J. Ng and A.W. Ackley, *Phys. Rev.* **D54** (1996), 4181;
 D.S. Lee, C.N. Leung and Y.J. Ng, *Phys. Rev.* **D 55** (1997) 6504;
 V.P. Gusynin and I.V. Shovkovy, *Phys. Rev.* **D 56** (1997) 5251;
 V.P. Gusynin, hep-ph/9709339.
- [7] E. Dagotto, A. Kocic and J.B. Kogut, *Phys. Rev. Lett.* **62** (1989), 1083; *Nucl. Phys.* **B334** (1990), 279.
- [8] K. Farakos and N.E. Mavromatos, preprint NTUA 67/97, OUTP-97-58P, cond-mat/9710288; *Int. J. Mod. Phys. B*, in press.
- [9] N. Dorey and N. E. Mavromatos, *Phys. Lett.* **B250** (1990), 107; *Nucl. Phys.* **B386** (1992), 614;
 For a comprehensive review of this approach see: N. Mavromatos, *Nucl. Phys. B* (Proc. Suppl.) 33C (1993), 145.
- [10] A. Kovner and B. Rosenstein, *Phys. Rev.* **B42** (1990), 4748.
- [11] K. Farakos and N.E. Mavromatos, *Phys. Rev.* **B57** (1998), 3017; preprint OUTP-97-36P, NTUA-65/97, hep-lat/9707027, *Mod. Phys. Lett. A* in press.
- [12] C.C. Tsuei *et al.*, *Phys. Rev. Lett.* **73** (1994), 593;
 K.A. Moler *et al.*, *Phys. Rev. Lett.* **73** (1994), 2744;
 D.A. Bonn *et al.*, *ibid.* **68** (1992), 2390.
- [13] P. W. Anderson, *Science* **235** (1987), 1196.
- [14] K. Krishana *et. al.*, *Science* **277** (1997), 83.
- [15] R.B. Laughlin, preprint cond-mat/9709004.
- [16] J. Schwinger, *Phys. Rev.* **82** (1951), 664.
- [17] I.S. Gradshteyn and I.M. Ryzhik, *Table of Integrals, Series, and Products* (Academic Press, New York 1980).